Eur. Phys. J. C 24, 459–468 (2002)
Digital Object Identifier (DOI) 10.1007/s10052-002-0964-4

THE EUROPEAN PHYSICAL JOURNAL C

Photon-exchange processes at hadron colliders as a probe of the dynamics of diffraction

V.A. Khoze[1,2], A.D. Martin[1], M.G. Ryskin[1,2]

[1] Department of Physics and Institute for Particle Physics Phenomenology, University of Durham, Durham, DH1 3LE
[2] Petersburg Nuclear Physics Institute, Gatchina, 188300 St. Petersburg, Russia

Received: 1 February 2002 / Revised version: 4 April 2002 /
Published online: 22 May 2002 –

Abstract. The rich structure of photon-exchange processes at hadron colliders is studied. We discuss central vector meson production ($pp \to p+J/\psi+p$), W production ($pp \to p+W+X$) and $\mu^+\mu^-$ production. Each process has distinct, and large, soft pp rescattering effects, which can be directly observed by detecting the outgoing protons. This allows a probe of the optical density of the proton, which plays a crucial role in the evaluation of the rapidity gap survival probabilities in diffractive-like processes at hadron colliders. We note that an alternative mechanism for J/ψ production is odderon, instead of photon, exchange; and that the ratio of odderon to photon contributions is enhanced (suppressed) for $\phi(\Upsilon)$ vector meson production.

1 Introduction

Processes with rapidity gaps at hadron colliders provide an attractive possibility (i) to search for New Physics (Higgs boson, SUSY particles, etc.) in a clean environment (see for example, [1] and references therein) and (ii) to study the properties of the diffractive amplitude. Unfortunately, the cross sections for such processes are suppressed by the small probability, $\hat{S}^2$, that the rapidity gaps survive soft rescattering effects between the interacting hadrons, which can generate secondary particles populating the gaps [2]–[9].

In general, we may write the survival factor $\hat{S}^2$ in a multi-channel eikonal framework in the form

$$\hat{S}^2 \;=\; \frac{\int \sum_i \left|\mathcal{M}_i(s,b_t^2)\right|^2 \exp\left(-\Omega_i(s,b_t^2)\right) d^2b_t}{\int \sum_i \left|\mathcal{M}_i(s,b_t^2)\right|^2 d^2b_t} \qquad (1)$$

where an incoming proton is decomposed into diffractive eigenstates, each with its own opacity[1] Ω_i. Here $\mathcal{M}_i(s,b_t^2)$ are the amplitudes (in impact parameter b_t space) of the process of interest at centre-of-mass energy $\sqrt{s}$. They may be different for the different diffractive eigenstates. It is important to note that the suppression factor $\hat{S}^2$ is not universal, but depends on the particular hard subprocess, as well as on the kinematical configurations of the parent reaction [9].

The opacities $\Omega_i(s,b_t)$ of the proton have been calculated in a number of models [12,10,11,8,9], and used to determine $\hat{S}^2$ for various rapidity gap processes. However it is difficult to guarantee the precision of predictions which rely on soft physics. The calculations of $\hat{S}^2$ can, in principle, be checked by computing the event rate for processes such as central Z production by WW fusion [4] or central dijet production with a rapidity gap on either side [13,10], and comparing with the experimental rate. However, to date, the only such check has been the prediction of the diffractive dijet production at the Tevatron in terms of the diffractive structure functions measured at HERA [9]. We may regard these as 'integrated' checks[2]. It is clearly desirable to study the *profile* of the optical density $\Omega(s,b_t^2)$ itself for some well known *observable* reaction, rather than simply the integrated quantity $\hat{S}^2$.

Here we show that central production processes mediated by photon exchange offer an excellent possibility to probe the opacity $\Omega(s,b_t^2)$ in more detail. The generic diagram for such a process is shown in Fig. 1a, together with the definition of the kinematic variables. For very small photon momentum transfer $t = q_1^2$, the scattering occurs at large impact parameters, outside the strong interaction radius, where the opacity is essentially zero, and $\hat{S}^2 \simeq 1$. As $|t|$ increases we probe smaller and smaller b_t and the opacity increases. In this way we can *scan* the opacity $\Omega(s,b_t^2)$. In terms of Feynman diagrams the rescattering induces interference between the contributions from Figs. 1a and 1b. Effectively, the $1/t$ form of the photon exchange amplitude is replaced by a more complicated form with a diffractive minimum in the region $|t| \sim 0.1$ GeV^2.

[1] Really we deal with a matrix $\Omega^{ii'}_{jj'}$, where the indices refer to the eigenstates of the two incoming and two outgoing hadrons [9]

[2] Another probe of the models for soft diffraction comes from the comparison of the experimental upper limit on the exclusive dijet production rate with the theoretical expectation [14]

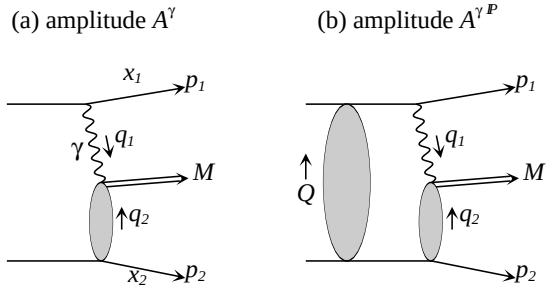

Fig. 1a,b. The exclusive $pp \to p + M + p$ process mediated by photon exchange **a** without and **b** with rescattering corrections. The particle four momenta are indicated. In this paper we take the system M to be the J/ψ vector meson, the W boson and, finally, a $\mu^+\mu^-$ pair. For W production we have, of necessity, proton dissociation at the lower vertex; that is $pp \to p+W+X$

To obtain the cleanest probe of this effect it is best to consider a reaction where the whole impact parameter distribution is driven by the photon propagator, while the amplitude for the γp subprocess samples a concentrated region, Δb_t, of the impact parameter space.

Moreover, we must study a process where photon exchange is a major contribution, and the background mechanisms are relatively small. One possibility is to observe the exclusive reaction

$$pp \ \to \ p \ + \ J/\psi \ + \ p, \tag{2}$$

where the + sign indicates the presence of a rapidity gap. To reduce the spread of Δb_t we should select events with relatively large momentum transfer ($p_{2t} \sim \mathcal{O}(1\ \text{GeV})$) in the quasi-elastic subprocess $\gamma p \to J/\psi + p$. Other examples are central W boson production via γW fusion and central $\mu^+\mu^-$ production via $\gamma\gamma$ fusion. That is the system M in Fig. 1 is either the J/ψ or the W boson or a massive $\mu^+\mu^-$ pair.

2 Rescattering in γ exchange proceses: a first look

To gain insight into how γ exchange processes allow a probe of the rapidity gap survival factor, we first perform a simplified evaluation of the diagrams of Fig. 1. As mentioned above we are interested in the regime where $p_{1t} \simeq 0-0.4$ GeV and $p_{1t}^2 \ll p_{2t}^2$. (One consequence is that the diagram with photon emission from the lower vertex is supressed.) To fix the $\gamma p \to Mp$ subprocess energy W we have to measure the longitudinal momentum fraction $\xi_1 = 1 - x_1$ carried by the photon, where x_1 is that of the detected proton.

In the small p_{1t} regime, the cross section, neglecting the rescattering contribution Fig. 1b, may be written in the factorized form

$$\sigma \ = \ \int dN(\xi_1)\, \sigma_{\gamma p \to Mp}(W), \tag{3}$$

where $N(\xi_1)$, the effective number of photons, is well known [15]. For small t it is safe to neglect longitudinally polarised photons and to consider only the number of transversely polarised photons. For $\xi_1 \ll 1$, neglecting terms of higher order in ξ_1 we have

$$dN^T(\xi_1) = \frac{d^2q_{1t}q_{1t}^2}{(q_{1t}^2+\xi_1^2m_N^2)^2}\ \frac{\alpha}{\pi^2}\ F_N^2(t) \times \left(1-\xi_1+\frac{1}{2}\xi_1^2\right)\ \frac{d\xi_1}{\xi_1}, \tag{4}$$

where, in the absence of rescattering $\vec{q}_{1t} = -\vec{p}_{1t}$. Here α is the QED coupling and the expression in brackets in the numerator is the QED splitting function for emission of a transversely polarised photon from the proton. The photon propagator can be written as

$$t \ = \ -\frac{\left(p_{1t}^2 \ + \ \xi_1^2 m_N^2\right)}{1 \ - \ \xi_1}, \tag{5}$$

where $|t_{\min}| = \frac{\xi_1^2 m_N^2}{1-\xi_1}$ and m_N is the proton mass. $F_N(t)$ is the electromagnetic form factor of the proton, which, in the simplified discussion presented in this section, we take to be $F_1(t)$. We may thus write the amplitude for Fig. 1a in the form

$$A^\gamma \ = \ \mathcal{M}\exp(-bq_{2t}^2/2)\ \left(\frac{q_{1t}}{q_{1t}^2+\xi_1^2m_N^2}\right)\ F_1(t), \tag{6}$$

where b is the slope of the differential cross section of the $\gamma p \to Mp$ subprocess, and $\mathcal{M}$ contains the W dependence of the subprocess, as well as the remaining ξ_1 dependence and other factors in (4).

To calculate the rescattering contribution, Fig. 1b, we use the momentum representation. Throughout the paper we neglect the rescattering of the system M, as it has a much smaller cross section. We may also neglect the spin flip component in the proton-Pomeron vertex[3]. To estimate the qualitative features of the rescattering effect we assume, in this Section, that the amplitude for elastic proton-proton scattering, at energy $\sqrt{s}$ and momentum transfer k_t, has the simplified form

$$A_{pp}(s,k_t^2) \ = \ A_0(s)\ \exp(-Bk_t^2/2). \tag{7}$$

From the optical theorem we have $\text{Im}A_0(s) = s\sigma_{pp}^{\text{tot}}(s)$, and for the small contribution of the real part it is sufficient to use $\text{Re}A_0/\text{Im}A_0 \simeq 0.13$ in the energy regime of interest. B is the slope of the elastic pp differential cross section, $d\sigma_{pp}/dt \propto \exp(Bt)$.

Using the above elastic pp amplitude we may write the rescattering contribution, Fig. 1b, to the $pp \to p + M + p$ amplitude as

$$A^{\gamma I\!P} = i\int \frac{d^2Q_t}{8\pi^2}\left(\frac{q_{1t}F_1(t)}{q_{1t}^2+\xi_1^2m_N^2}\right) \times\mathcal{M}\exp(-bq_{2t}^2/2 - BQ_t^2/2)\ \frac{A_0(s)}{s} \tag{8}$$

[3] This component is expected to be small and consistent with zero. If we note the similarity between the photon and Pomeron vertices then the magnitude of the isosinglet spin-flip amplitude is proportional to $\left|\frac{1}{2}(\mu_p^a+\mu_n^a)\right| \lesssim 0.06$, where the anomalous magnetic moments μ^a of the neutron and proton cancel each other almost exactly

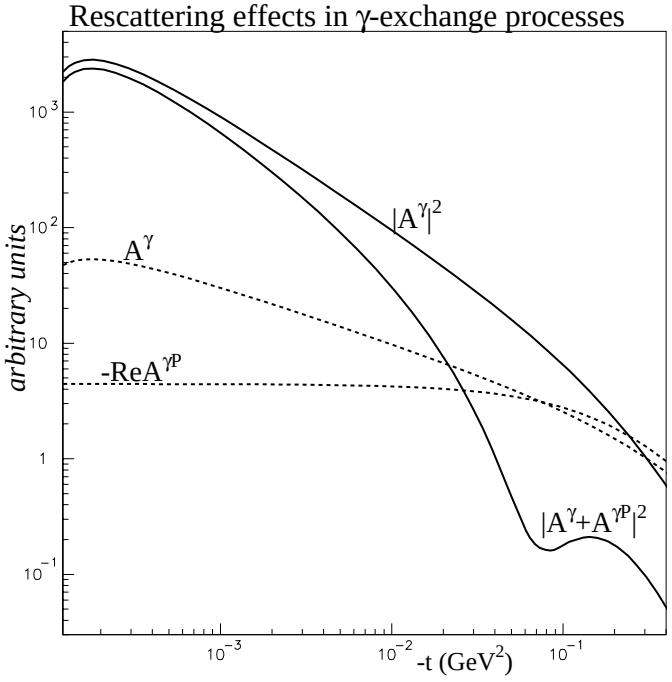

Fig. 2. The cross sections, $|A^\gamma|^2$ and $|A^\gamma + A^{\gamma\mathbb{P}}|^2$, for the γ-exchange process $pp \to p + M + p$ of Fig. 1, without and with rescattering corrections respectively. The dashed curves show the contributing amplitudes calculated from (6) and (8), in the simple case with slope $b = 0$. For the elastic proton-proton amplitude, A_{pp}, we take (7) with slope $B = 17$ GeV^{-2} and $\sigma_{pp}^{\rm tot} = 76$ mb, which correspond to the Tevatron measurements [16]

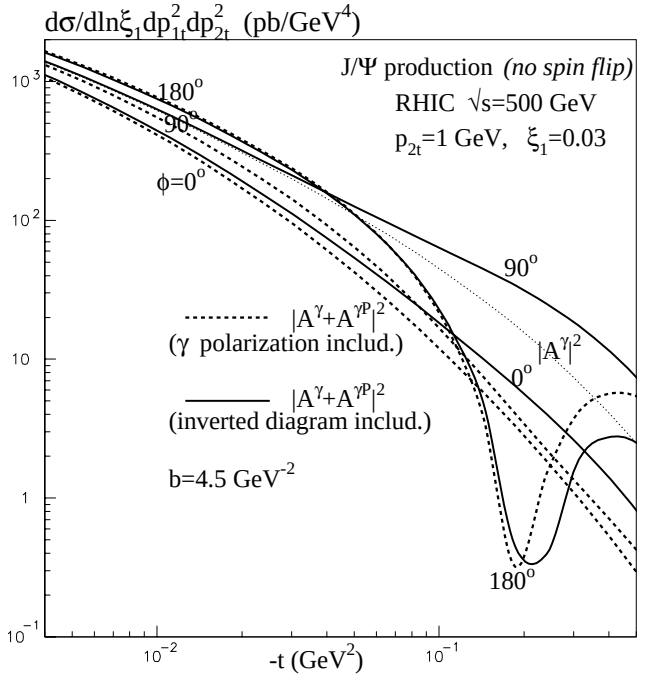

Fig. 3. The differential cross section for $pp \to p + J/\psi + p$ via photon exchange at $\sqrt{s} = 500$ GeV. The dashed curves include rescattering, with a proper treatment of photon polarisation. The solid curves also include, besides the amplitudes of Fig. 1, the 'inverted' amplitudes with the photon coupled to the lower proton. The predictions are shown for three values of the azimuthal angle, $\phi = 0°, 90°, 180°$, between the transverse momenta $\vec{p}_{1t}$ and $\vec{p}_{2t}$ of the outgoing protons. Here and in what follows t is given by (5)

with

$$\vec{q}_{1t} \;=\; \vec{Q}_t - \vec{p}_{1t}, \qquad -\vec{q}_{2t} \;=\; \vec{Q}_t + \vec{p}_{2t}. \tag{9}$$

The photon induced singularity ($\sim 1/q_{1t}$ for $\xi_1 \to 0$) is integrable in (8). The main contribution comes from the region $Q_t^2 \sim 2/B$. For small $p_{1t}^2 \ll (p_{2t}^2, 2/B)$, the Q_t integration may be performed, and we find

$$A^{\gamma\mathbb{P}} \;\sim\; i\,\frac{A_0(s)}{8\pi s}\mathcal{M}\sqrt{\frac{2\pi}{(B+b)}}\;\exp\left(-\frac{bB}{2(b+B)}\,p_{2t}^2\right). \tag{10}$$

The effect of rescattering is shown in Fig. 2. Here, for simplicity, we have set the slope $b = 0$, that is the $\gamma p \to Mp$ subprocess is assumed to occur at zero impact parameter. The upper curve, $|A^\gamma|^2$, is proportional to the cross section for the photon-mediated process $pp \to p + M + p$ of Fig. 1a in the absence of rescattering, whereas the $|A^\gamma + A^{\gamma\mathbb{P}}|^2$ curve shows the effect of including the rescattering corrections of Fig. 1b. The diffractive dip in the region of $-t \sim 0.1$ GeV^2, due to the destructive interference of the A^γ and $A^{\gamma\mathbb{P}}$ amplitudes, is clearly evident. The dip is partially filled in by the presence of the $\mathrm{Re}A_0$ contribution to (7), which leads to a small $\mathrm{Im}A^{\gamma\mathbb{P}}$ term. It is clear that a measurement of the t dependence of the cross section will provide a scan of the rapidity gap survival probability $\hat{S}^2$, that is of the proton optical density $\Omega(s, b_t^2)$. It is seen that rescattering gives more than an order of magnitude suppression in the region $0.03 \lesssim -t \lesssim 0.2$ GeV^2.

So far we have considered only the amplitude which conserves the s-channel proton helicity at the vertex with the exchanged photon. This non-flip amplitude is described by the $F_1(t)$ electromagnetic form factor of the proton. However as $-t$ increases the helicity at the photon vertex may be flipped by the proton's anomalous magnetic moment. The spin-flip amplitude is described by the form factor $F_2(t)$. Neglecting terms of order ξ_1^2 the amplitude is given by an expression analogous to (6), with $F_1(t)$ replaced by $(q_{1t}/2m_N)F_2(t)$. In almost all of the results presented below we include the spin-flip contribution, although, for simplicity, we write the formulae in terms of the non-flip amplitude alone. The exception is Fig. 3. The comparison of Fig. 3 with Fig. 4 shows that the effect of the spin-flip contribution is quite small.

3 Second look: inclusion of photon polarisation

So far we have studied photon-exchange reactions in hadron colliders with the neglect of photon polarisation, as is often done in the equivalent photon approach. However, when we include soft pp rescattering effects, we must take care. Frequently for photon exchange processes we deal with expressions of the form

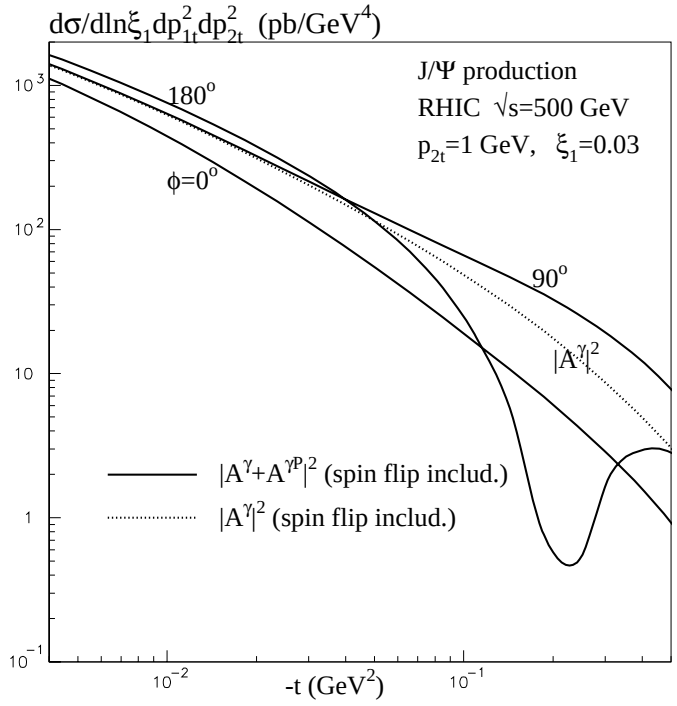

Fig. 4. The continuous curves are as in Fig. 3 but with the proton spin-flip amplitude included

$$|A|^2 \;=\; \vec{\varepsilon}\cdot\vec{\varepsilon}^{\,\prime *}|T|^2, \tag{11}$$

where $\vec{\varepsilon}$ and $\vec{\varepsilon}^{\,\prime *}$ are the photon polarisation vectors of the amplitude and the complex conjugate amplitude respectively. At small ξ_1 the polarisation vector $\vec{\varepsilon}$ is aligned with the transverse momentum $\vec{q}_{1t}$. We take $\vec{\varepsilon}$ in the direction $-\vec{q}_{1t}$. Without rescattering, Fig. 1a, we have $\vec{q}_{1t} = -\vec{p}_{1t}$, whereas for the rescattering contribution, Fig. 1b, we have $\vec{q}_{1t} = \vec{Q}_t - \vec{p}_{1t}$. In the latter case we see that the photon polarisation depends on the loop momentum $\vec{Q}_t$, and so we must work in terms of the two different polarisation states. It is convenient to choose a linear polarisation basis. We take one polarisation vector $\vec{\varepsilon}_1$ aligned with $\vec{p}_{1t}$ (which is the polarisation vector of the photon in the absence of rescattering), and the other, $\vec{\varepsilon}_2$, perpendicular to $\vec{\varepsilon}_1$. The amplitude A^γ of Fig. 1a proceeds only via the first polarisation vector and hence the $pp \to p + M + p$ cross section via γ-exchange has the form

$$\sigma \;\propto\; |A^\gamma + A_1^{\gamma\mathbb{P}}|^2 \;+\; |A_2^{\gamma\mathbb{P}}|^2. \tag{12}$$

Let us study the impact of $\vec{\varepsilon}\cdot\vec{\varepsilon}^{\,\prime *}$ on the interference term between the amplitudes A^γ and $A^{\gamma\mathbb{P}}$. In general, we have

$$A^\gamma A^{\gamma\mathbb{P}*} \;\sim\; -\vec{\varepsilon}_1\cdot\vec{\varepsilon}^{\,\prime *} \;\sim\; -\vec{p}_{1t}\cdot(\vec{p}_{1t} - \vec{Q}_t), \tag{13}$$

where the minus sign arises because $A^{\gamma\mathbb{P}}$ is negative relative to A^γ due to the absorptive nature of Pomeron exchange. For very small values of p_{1t} we see that $\vec{\varepsilon}^{\,\prime}$ is antiparallel to $\vec{Q}_t$. Moreover, the main contribution of Fig. 1b comes from the smaller values of q_{2t}, and so $\vec{Q}_t$ tends to be antiparallel to $\vec{p}_{2t}$. Hence $\vec{\varepsilon}^{\,\prime}$ tends to be parallel to $\vec{p}_{2t}$, and

$$A^\gamma A^{\gamma\mathbb{P}*} \sim -\vec{\varepsilon}_1\cdot\vec{\varepsilon}^{\,\prime *} \sim -\vec{p}_{1t}\cdot\vec{p}_{2t} \quad \text{(for very small } p_{1t}\text{)}. \tag{14}$$

On the other hand, as p_{1t} increases, $\vec{\varepsilon}^{\,\prime}$ becomes more and more parallel to $\vec{p}_{1t}$. Hence

$$A^\gamma A^{\gamma\mathbb{P}*} \sim -\vec{\varepsilon}_1\cdot\vec{\varepsilon}^{\,\prime *} \sim -\vec{p}_{1t}\cdot\vec{p}_{1t} \quad \text{(for larger } p_{1t}\text{)}. \tag{15}$$

From (14) we see that the interference term depends on the azimuthal angle ϕ between the transverse momenta of the outgoing protons, $\vec{p}_{1t}$ and $\vec{p}_{2t}$. For very small $\vec{p}_{1t}$, we have *constructive* interference if $\vec{p}_{1t}$ and $\vec{p}_{2t}$ are back-to-back (that is if $\phi = 180°$), and *destructive* interference when $\vec{p}_{1t}$ and $\vec{p}_{2t}$ are aligned ($\phi = 0$). As p_{1t} increases, $\vec{\varepsilon}^{\,\prime}$ becomes more and more aligned with $\vec{p}_{1t}$, rather than $\vec{p}_{2t}$, and we have destructive interference for all azimuthal angles ϕ, see (15).

The evaluation of the exclusive process $pp \to p + J/\psi + p$ is described in Sect. 5. However it is informative to show a sample of these results now, in order to illustrate the effects of including the proper treatment of the photon polarisation. Figure 3 shows the differential cross section at energy $\sqrt{s} = 500$ GeV appropriate to RHIC for a realistic choice of kinematic variables. The (dotted) reference curve, denoted by $|A^\gamma|^2$, is the naive estimate based on Fig. 1a. It was obtained by multiplying the $\gamma p \to J/\psi + p$ cross section by the equivalent photon flux, (3). For simplicity here we neglect the contributions which flip the spin of the proton. The other curves in Fig. 3 show the effect of including the rescattering contribution of Fig. 1b. We take a realistic slope $b = 4.5$ GeV^{-2} for the $\gamma p \to J/\psi + p$ subprocess, as described in Sect. 5.

The dashed curves in Fig. 3 show the predictions for the $pp \to p + J/\psi + p$ cross section which include the correct treatment of the photon polarisation, for three different choices of the azimuthal angle, namely $\phi = 0, 90°$ and 180°. These results clearly demonstrate the anticipated behaviour obtained in (14) and (15). For $\phi = 180°$ the rescattering amplitude $A^{\gamma\mathbb{P}}$ has the largest absolute value. It is positive for small $-t$ and reverses sign as $-t$ increases. As a consequence, the diffractive dip is deeper and narrower than the simple prediction shown in Fig. 2. For $\phi = 0$ and 90° the amplitude $A^{\gamma\mathbb{P}}$ is negative everywhere and relatively smaller, which shifts the respective dips outside the region of interest.

Besides, allowing for the effects of photon polarisation, there is another complication that we must consider. As $-t$ increases, we have to include the contributions of diagrams analogous to those shown in Fig. 1, but with the photon and Pomeron exchanges interchanged. That is we must include contributions from 'inverted' diagrams with the photon coupled to the lower proton vertex. Their contribution is negligibly small for very small q_{1t} and larger values of ξ_1, but increases significantly in the dip region. The results obtained after including these extra amplitudes are shown by the three continuous curves in Fig. 3. It is interesting to note that for $\phi = 90°$ the extra diagrams have a large effect in the region where p_{1t} becomes

comparable to p_{2t}, and lead to a cross section even larger than that due to the reference $|A^\gamma|^2$ prediction in the absence of rescattering.

4 Detailed formalism for rescattering corrections

Before we consider specific examples of $pp \to p + M + p$ production via photon exchange, we describe a more realistic way to evaluate rescattering corrections than that described in Sect. 2. We use the formalism and the results of [11]. The formalism embodies (i) pion-loop insertions to the Pomeron trajectory, (ii) two-channel eikonal description of proton-proton rescattering and (iii) high mass diffractive dissociation. The parameters of the model were tuned to describe all the main features of the soft pp data throughout the CERN-ISR to the Tevatron energy interval. In terms of the two-channel eikonal the incoming proton is described by two diffractive eigenstates $|\phi_i\rangle$, each with its own absorptive cross section.

The eigenstates were taken to have the same profile in impact parameter space, and absorptive cross sections

$$\sigma_i \;=\; a_i\sigma_0 \qquad \text{with} \qquad a_i \;=\; 1 \pm \gamma, \tag{16}$$

where $\gamma = 0.4$ [11]. That is the two channel opacity is

$$\Omega_{jj'}^{ii'} \;=\; \delta_{ii'}\delta_{jj'}a_i a_j \Omega. \tag{17}$$

The impact parameter representation of the elastic amplitude is thus

$$\frac{1}{s}\,\mathrm{Im}\,\tilde{A}_{pp}(b_t) = \Big(1 - \frac{1}{4}\Big[e^{-(1+\gamma)^2\Omega/2} + 2e^{-(1-\gamma^2)\Omega/2} + e^{-(1-\gamma)^2\Omega/2}\Big]\Big). \tag{18}$$

As both the eigenstates $|\phi_i\rangle$ have the same b_t profile, photon emission is controlled by the same proton electromagnetic form factors $F_1(t)$ and $F_2(t)$, and there are no off-diagonal transitions at the photon vertex

$$\langle\phi_1|\gamma|\phi_2\rangle \;=\; \langle\phi_2|\gamma|\phi_1\rangle \;=\; 0. \tag{19}$$

Therefore the amplitude of pp rescattering, which occurs in Fig. 1b, takes the form

$$\mathrm{Im}\,\tilde{A}_{pp}(s,b_t) = s\Big(1 - \frac{1}{4}\Big[(1+\gamma)e^{-(1+\gamma)^2\Omega/2} + 2e^{-(1-\gamma^2)\Omega/2} + (1-\gamma)e^{-(1-\gamma)^2\Omega/2}\Big]\Big). \tag{20}$$

The extra $(1 \pm \gamma)$ factors reflect the different Pomeron couplings to the $|\phi_i\rangle$ eigenstates in the $pp \to p + M + p$ production amplitude, that is in the right-hand part of Fig. 1b. The optical density $\Omega(s, b_t)$ was given in [11] for Tevatron ($\sqrt{s} = 2$ TeV) and LHC ($\sqrt{s} = 14$ TeV) energies.

As before, we work in momentum space, and replace (7) by

$$A_{pp}(s,k_t^2) \;=\; \frac{1}{2\pi}\int d^2b_t\, 4\pi\, \tilde{A}_{pp}(s,b_t)\, e^{i\vec{k}_t\cdot\vec{b}_t}. \tag{21}$$

Hence the amplitude of Fig. 1b becomes

$$A^{\gamma\mathbb{P}} = -\int \frac{d^2Q_t}{8\pi^2}\left(\frac{q_{1t}F_1(t)}{q_{1t}^2 + \xi_1^2 m_N^2}\right)\frac{A_{pp}(s,Q_t^2)}{s} \;\mathcal{M}\,\exp(-bq_{2t}^2/2), \tag{22}$$

in analogy to (8). The amplitude $\mathcal{M}$ is defined below (6). Although here we show only Im A_{pp}, we include the contribution from Re A_{pp} as described in Sect. 2.

5 Exclusive J/ψ hadroproduction mediated by γ exchange

Here we study the photon-mediated exclusive reaction, $pp \to p + J/\psi + p$ of Fig. 1, in more detail. The cross section of the $\gamma p \to J/\psi + p$ subprocess may be calculated perturbatively (see, for example, [17–19]) or taken from extrapolations of the HERA data [20]. The cross section is well described by

$$\frac{d\sigma}{dt_2}(\gamma p \to J/\psi + p) \;\simeq\; 70\ \mathrm{nb}\left(\frac{W}{100\ \mathrm{GeV}}\right)^{0.83} e^{bt_2}, \tag{23}$$

with slope $b \simeq 4.5\ \mathrm{GeV}^{-2}$, practically independent of the centre-of-mass energy W.

To a good approximation, s-channel helicity is conserved in the $\gamma p \to J/\psi + p$ process and, for small q_{1t}^2, the amplitudes $\mathcal{M}_{\lambda_\gamma,\lambda_\psi}$ satisfy

$$\left|\frac{\mathcal{M}_{00}}{\mathcal{M}_{11}}\right|^2 \;\sim\; \mathcal{O}\left(\frac{q_{1t}^2}{M_\psi^2}\right). \tag{24}$$

Thus, for the small values of q_{1t}^2 of interest here, it is safe to neglect production via longitudinally polarized photons.

Now the full calculation of the differential cross section for the exclusive process $pp \to p + J/\psi + p$ via photon exchange goes well beyond the equivalent photon approach described in Sect. 2. First we must allow for the proper treatment of the photon polarisation as discussed in Sect. 3. Then we must include the amplitudes of inverted diagrams, analogous to those in Fig. 1 but with the photon coupled to the lower proton. Figure 4 shows the final result for a realistic RHIC configuration. The effect of rescattering is clearly pronounced in the region $-t \sim 0.1\ \mathrm{GeV}^{-2}$, and displays a rich ϕ dependence. Recall, ϕ is the azimuthal angle between the transverse momenta, $\vec{p}_{1t}$ and $\vec{p}_{2t}$, of the outgoing protons. The cross section is sizeable. For example, in a typical bin, $\Delta p_{1t}^2 \sim 0.02\ \mathrm{GeV}^2, \Delta p_{2t}^2 \sim 0.2\ \mathrm{GeV}^2$ and $\Delta \ln \xi_1 \sim 1$, we expect more than 0.1 pb for $-t \sim 0.1\ \mathrm{GeV}^2$. However the $J/\psi \to \mu^+\mu^-$ branching ratio has not been included.

In Fig. 5 we present the analogous results for $p\bar{p}$ collisions[4] at the Tevatron energy $\sqrt{s} = 2$ TeV. To demonstrate the sensitivity of the differential cross section to

[4] Note that for $p\bar{p}$ collisions the 'inverted' diagrams enter with the opposite sign

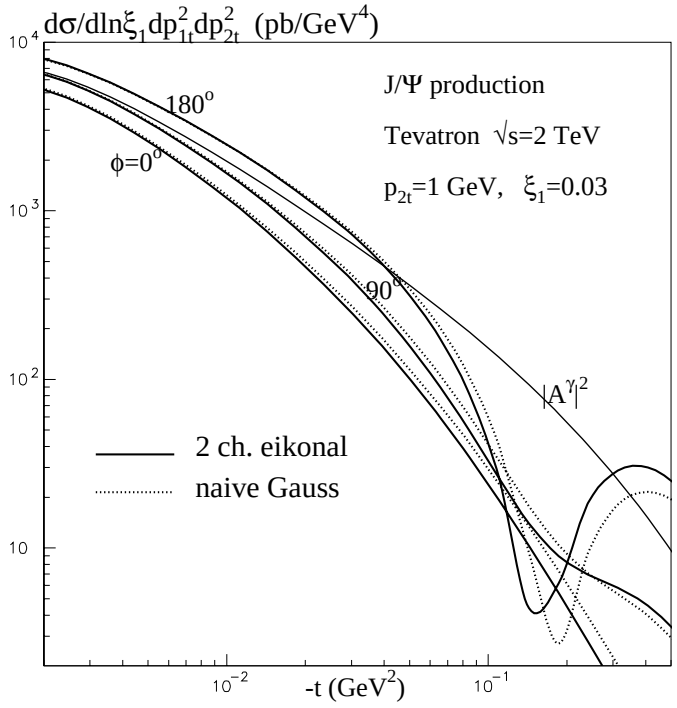

Fig. 5. As in Fig. 3, but for $p\bar{p} \to p + J/\psi + \bar{p}$ at $\sqrt{s} = 2$ TeV. The dotted curves correspond to the simple pp rescattering amplitude described in Sect. 2

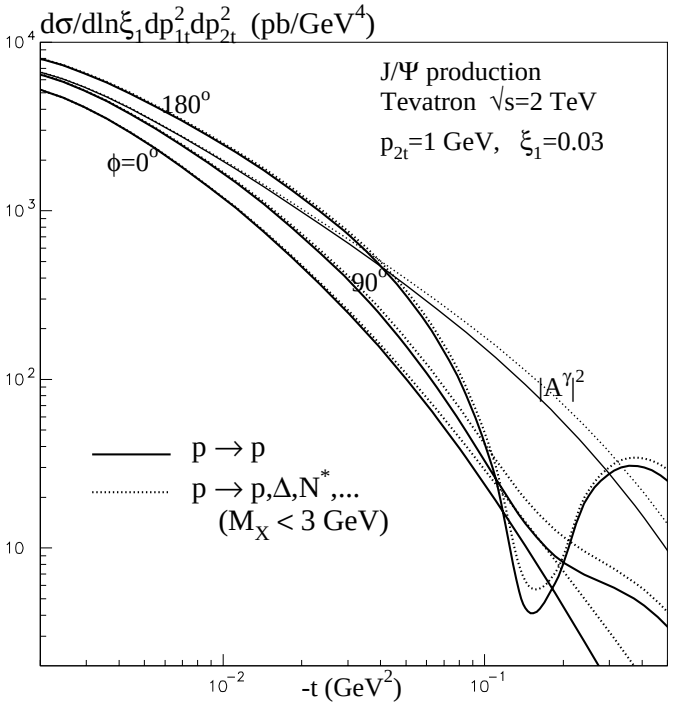

Fig. 6. As in Fig. 5, but here the dotted curves allow for excitations up to mass 3 GeV of the unobservable proton

the profile of the proton opacity, we compare the results obtained using the two-channel eikonal model [11], described in Sect. 4, with the values calculated using the simple pp Gaussian amplitude of (7) with the same slope $B = 17$ GeV^{-2} and $\sigma_{pp}^{\rm tot} = 76$ mb that appear in the two-channel eikonal model. Unfortunately, for the reasons we now discuss, it will be difficult to observe $p\bar{p} \to p + J/\psi + \bar{p}$ at the Tevatron.

6 Observability of $pp \to p + J/\psi + p$

It is clearly important to measure the kinematic variables $\vec{p}_{it}$ and $x_i = 1 - \xi_i$ of the outgoing protons. To study photon-exchange reactions we require a proton at very small transverse momentum, say $\vec{p}_{1t}$. Unfortunately it is not possible to measure very small $\vec{p}_{it}$ and ξ_i simultaneously since, in this case, an outgoing proton scatters into the beam pipe. Thus we choose $p_{2t} \sim 1$ GeV/c and $\xi_1 > 0.01$. Indeed, in practice it might be necessary to have $\xi_1 > 0.05$. It is also necessary to identify the J/ψ vector meson, so as to be sure that we have negative C parity production (and do not replace photon by Pomeron exchange).

In principle, with very good resolution, it would be possible to observe J/ψ as a peak in the missing mass spectrum. In practice, this will be extremely difficult. Thus we need to observe the decay $J/\psi \to \mu^+\mu^-$. (Note that the branching fraction for this decay is not included in the results that we present.) For Tevatron energies, however, with $\xi_1 = 0.05$, the muons are emitted at very small centre-of-mass angles, less than 3°. Therefore in Sect. 3 we presented predictions for RHIC energies, where the situation is better.

Another possibility is to measure only one recoil proton with $p_{2t} \sim 1$ GeV/c and to observe the J/ψ. Then $\vec{p}_{1t}$ may be deduced as $-(\vec{p}_{2t} + \vec{p}_{\psi t})$. However there may be some inelastic contribution from processes in which the undetected proton is knocked into an excited state. This contribution can be calculated when the upper limit for the mass of the excitation is specified. Qualitatively, the contribution of the excited states acts as if it were described by a spin-flip amplitude, which does not interfere with the main non-flip contribution.

To demonstrate the possible effect, we show in Fig. 6 the prediction which includes the excitation of the unobservable proton into Δ and N^* resonances up to mass $M = 3$ GeV. We see that the additional contribution does not spoil the rich t and ϕ dependence of the differential cross section.

There is a potential background for $pp \to p + J/\psi + p$ process coming from double-Pomeron χ production, $pp \to p + \chi + p$ with $\chi \to J/\psi + \gamma$. The cross section for $\chi_c(0^{++})$ production at the Tevatron has been estimated to be $d\sigma/dy \sim 120$ nb [7]. That is $d\sigma/dy dp_{1t}^2 dp_{2t}^2 \sim 20-40$ nb/GeV^4 at $-t \sim 0.1$ GeV^2. The $\chi(0^{++}) \to J/\psi + \gamma$ branching fraction is 0.007, so the background is a few times larger than the signal. Thus, with a J/ψ mass resolution no better than 0.4 GeV, it is necessary to observe the γ from χ decay. The $\chi(2^{++})$ and $\chi(1^{++})$ states have much larger $J/\psi + \gamma$ branching fractions, but much smaller production cross sections and give less background than $\chi(0^{++})$.

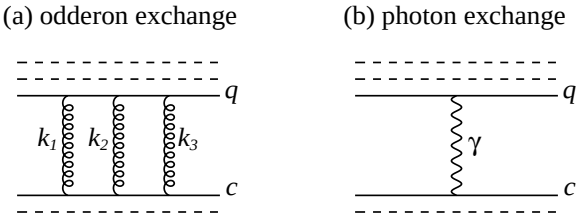

Fig. 7a,b. The comparison of the **a** odderon- and **b** photon-exchange contributions to the quark-(charm)quark amplitude, which are relevant for the process $pp \to p{+}J/\psi{+}p$. The spectator quarks are shown by the dashed lines, and all permutations of the gluons coupling to different quarks are implied

7 J/ψ production via odderon exchange

In principle, the process $pp \to p + J/\psi + p$ may also be mediated by odderon exchange [21]. That is the photon in Fig. 1 may be replaced by a three-gluon t-channel state, where each pair of gluons form a symmetric colour octet, 8_s. Such a three-gluon state has negative C-parity and describes odderon exchange. Little is known about the odderon amplitude. So far, the odderon has not been seen experimentally. There are indications that the odderon-nucleon coupling is small [22]. In particular, the coupling is zero in the specific model in which the nucleon is made up of a quark and a (point-like) diquark.

At leading $\alpha_S \ln s$ order the intercept of the odderon trajectory is predicted to be very close to 1 [23]. From this point of view a single three-gluon exchange amplitude appears as a natural model for the odderon. For the quark-(charm)quark interaction, shown in Fig. 7, the amplitude is

$$T_{qc} = \frac{10\alpha_S^3}{81\pi} \int \frac{d^2k_{1t}}{k_{1t}^2} \frac{d^2k_{2t}}{k_{2t}^2} \frac{d^2k_{3t}}{k_{3t}^2} \delta^{(2)} \times \left(\vec{q}_t - \vec{k}_{1t} - \vec{k}_{2t} - \vec{k}_{3t}\right). \quad (25)$$

For the case of interest, $\xi_1 \ll 1$, we have $k_i^2 \simeq -k_{it}^2$, q_t is the total momentum transferred by the odderon. The numerical factor $10/81\pi$ arises from (i) the symmetry of the gluons (1/3!), (ii) the sum over the gluon colour indices ($\sum |d_{abc}|^2 = 40/3$), (iii) averaging over the colours of the incoming quarks, and (iv) $1/2\pi$ from the Feynman loop integration.

Figure 7 is not the only, or necessarily the largest[5], odderon exchange contribution to $pp \to p + J/\psi + p$. However it should give a reasonable preliminary order-of-magnitude estimate of the possible magnitude of odderon-exchange. For such an estimate we take amplitude (25) with an appropriate infrared cut-off given by the size of the J/ψ meson; $k_0 = 1/m_c$, and assume quark additivity. That is, we assume the coupling of the odderon to the (upper) proton is three times the odderon-quark coupling. Then the odderon-exchange contribution to the proton-charm quark amplitude is

$$T_{pc}^{\text{odderon}} \sim 3\,\frac{10\alpha_S^3}{81\pi}\left(\frac{15\pi^2}{m_c^2}\right) \sim 1\ \text{GeV}^{-2}, \quad (26)$$

using $\alpha_S \sim 0.5$, as compared to the photon-exchange contribution

$$T_{pc}^{\gamma} = \frac{4\pi\alpha}{q_t^2}\,2e_c = \frac{0.12}{q_t^2} \quad (27)$$

with the charge of the charm quark $e_c = 2/3$. The expression in brackets in (26) is the estimate of the integral in (25) with cut-offs $k_{it} > m_c$[6]. Comparing (26) and (27), it is evident that photon exchange dominates for very small q_t^2, but already by $q_t^2 \sim 0.1\ \text{GeV}^2$ odderon-exchange may become of comparable importance.

It may be possible to use ϕ or Υ vector meson production to distinguish between odderon and γ exchange. If we compare Υ to J/ψ production, then see that the odderon amplitude is suppressed by $1/m_b^2$ as compared to $1/m_c^2$. However the $pp \to p + \Upsilon + p$ rate via photon-exchange, times the $\Upsilon \to \mu^+\mu^-$ branching fraction, is more than three orders of magnitude smaller than for J/ψ production, and so the signal will be difficult to observe.

On the other hand, the cross section for ϕ production, via photon-exchange, exceeds J/ψ by a factor of 20, and so it should be possible to observe the $\phi \to K\bar{K}$ and $\mu^+\mu^-$ decay modes. Here the relative magnitude of the photon-exchange amplitude is suppressed by the strange quark charge ($e_s = -1/3$), while the odderon is enhanced by the large size of the ϕ meson. Therefore exclusive ϕ production appears to be a promising way to search for the odderon.

Finally, intrinsic charm [24] is another potential mechanism for the process $pp \to p + J/\psi + p$. However it is unlikely that there is enough intrinsic charm component in the proton at small ξ_1. The mechanism is to replace photon exchange by a $c\bar{c}$ pair in the t-channel. Such an amplitude dies out linearly with ξ_1 (modulo logarithmic corrections) as compared to photon-exchange contribution. The lowest order perturbative QCD estimate gives a contribution an order-of-magnitude smaller than odderon exchange.

8 W boson hadroproduction via γ exchange

Another possible way to investigate rescattering effects is central W production in the process $pp \to p + W + X$, where the W boson is separated from the dissociating proton by a large rapidity gap, $\Delta\eta$. The leading contribution comes from the diagram shown in Fig. 8a. Other configurations where the exchanged photon interacts with a quark emitting the W boson, rather than directly with the W, are suppressed by a factor $\exp(-\Delta\eta)$. (A possible odderon-exchange contribution would be suppressed by the same factor, as gluons cannot couple to the W

[5] There is also the probability that one of the three t-channel gluons could couple directly to the lower proton rather than to the c quark and, together with another t-channel gluon, forms a Pomeron in the lower part of the diagram for the $pp \to p + J/\psi + p$ process

[6] Technically, for each k_{it} below m_c, the integrand in (25) is multiplied by an additional factor k_{it}/m_c

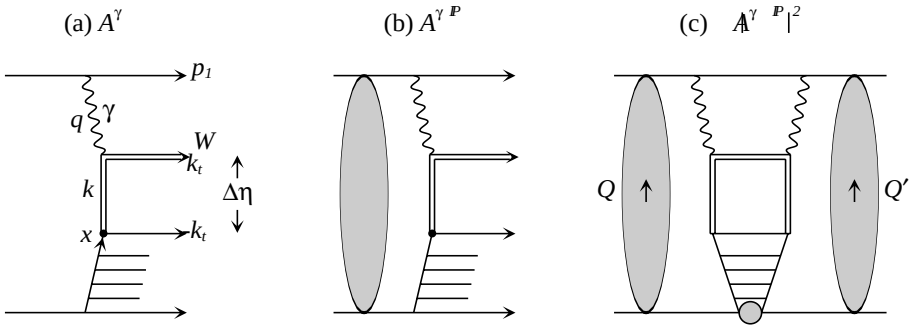

Fig. 8a–c. Photon-exchange amplitude for the process $pp \to p + W + X$, **a** without, and **b** with, rescattering effects. Diagram **c** shows the rescattering amplitude times its complex conjugate

boson.) Our predictions below are based on the leading configuration.

The cross section corresponding to the diagram of Fig. 8a may be written as

$$d\sigma \;=\; dN^T \sigma(\gamma p \to W + X), \tag{28}$$

where the effective number of photons N^T is given by (4), and

$$\sigma(\gamma p \to W + X) = \int_{x_{\min}}^{1} \frac{dx}{x}\, U(x) \frac{g^2 \alpha}{4} \times \frac{(1 + k_t^2/2M_W^2)}{(M_W^2 + k^2)^2}\, dk_t^2, \tag{29}$$

where k_t^2 is the square of the momentum transferred through the t-channel W boson and $g^2 = 8M_W^2 G_F/\sqrt{2}$. The density of quarks which may emit the W^+ boson is

$$U(x) = xu(x,k_t^2) + x\bar{d}(x,k_t^2) + x\bar{s}(x,k_t^2) + xc(x,k_t^2). \tag{30}$$

For W^- production, $U(x)$ is replaced by

$$D(x) = x\bar{u}(x,k_t^2) + xd(x,k_t^2) + xs(x,k_t^2) + x\bar{c}(x,k_t^2). \tag{31}$$

The minimal momentum fraction $x_{\min}$ carried by the parent quark is limited by the requirement that the recoil quark jet with transverse momentum k_t be outside the rapidity gap $\Delta\eta$, that is[7]

$$x_{\min} = \sqrt{\frac{M_W^2 + k_t^2}{s}}\, \exp(-y) \;+\; \frac{k_t}{\sqrt{s}}\, \exp(-y + \Delta\eta), \tag{32}$$

where $y = \frac{1}{2} \ln\left((E + k_z)/(E - k_z)\right)$ is the W boson rapidity. The two terms in the expression in brackets in the numerator in (29) correspond to the production of transversely and longitudinally polarised W bosons.

The amplitude with rescattering $A^{\gamma I\!P}$, Fig. 8b, has a form similar to (22). Again we allow for photon polarisation effects. However, now there is almost no correlation between Q_t and k_t, as the relatively small loop momentum Q_t is separated from the W transverse momentum k_t by a long evolution chain. The only novel point is that in the rescattering term squared, $|A^{\gamma I\!P}|^2$, the loop momenta Q_t and Q_t' (corresponding to the complex conjugate amplitude) are correlated via Fig. 8c by the form factor $\exp\left(-b_N(\vec{Q}_t + \vec{Q}_t')^2\right)$. The slope b_N, associated with the proton-Pomeron vertex, characterises the spatial distribution of the quarks in the proton before the DGLAP evolution. Note that for $pp \to p + W + X$, as one proton dissociates, there are no complications from 'inverted' diagrams.

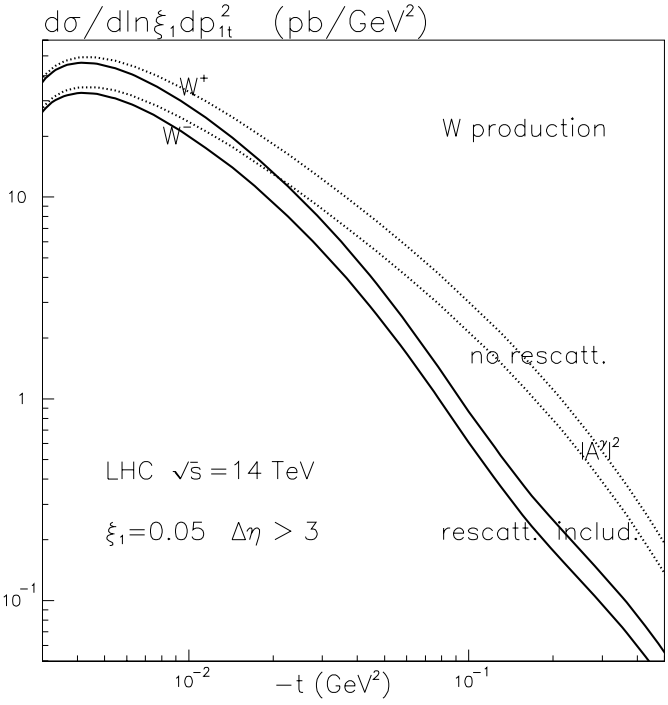

Fig. 9. The differential cross section for $pp \to p + W^\pm + X$ at the LHC. The dotted and continuous curves correspond, respectively, to the predictions without and with the rescattering effects of Figs. 8b,c. In each case W^+ production corresponds to the upper one of the pair of curves. The rapidity gap between the quark recoil jet and the W boson is taken to satisfy $\Delta\eta > 3$

Sample results for the $pp \to p + W^\pm + X$ differential cross sections at the LHC energy are shown in Fig. 9. The dotted and continuous curves correspond to the results without, and with, rescattering effects respectively. As the azimuthal angle ϕ has been integrated over the diffractive dip, which was clearly visible at $\phi = 180°$ for $pp \to p +$

[7] In the case of recoil charm-quark jet we substitute k_t in the second term in (32) by $\sqrt{k_t^2 + m_c^2}$

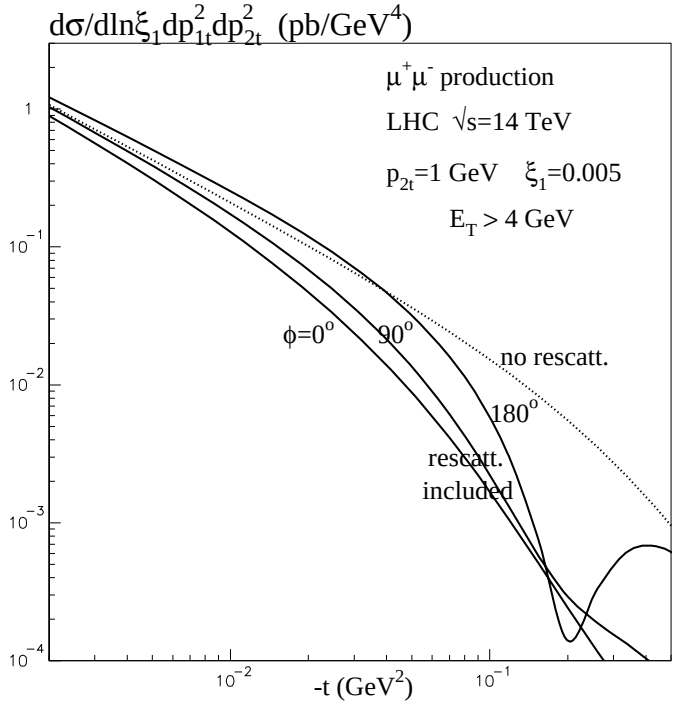

Fig. 10. The cross section for $pp \to p+(\mu^+\mu^-)+p$ at the LHC energy, with (continuous curves) and without (dotted curve) rescattering effects included. The rescattering effects are shown for three values of the azimuthal angle ϕ between the transverse momenta, $\vec{p}_{1t}$ and $\vec{p}_{2t}$, of the outgoing protons

$J/\psi + p$, is now very shallow. We see that rescattering suppresses the cross section by a factor of about 4 for $-t \sim 0.1$ GeV^2. The rescattering is calculated using the prescription of [11]. If the more complicated model of [9] is used, then we find the predictions change by less than 10%, the effect is maximal in the region of the dip ($|t| \sim 0.1$ GeV^2), where the rate rises by about 10%.

Of course, the process is hard to observe in the $W \to q\bar{q}$ decay mode, due to the huge QCD background. However, the cross section is large enough to be observed in the leptonic decay modes. For example, from Fig. 9 we see that the $\Delta p_{1t}^2 \simeq 0.03$ GeV^2, $\Delta \ln \xi_1 \simeq 1$ bin at $-t \sim 0.1$ GeV^2 has a cross section of about 20 fb. If the momenta of the charged lepton, the outgoing proton and the recoil jet can be measured, then we can reconstruct the mass of the W boson.

9 $\mu^+\mu^-$ pair production via $\gamma\gamma$ fusion

The exclusive process $pp \to p + (\mu^+\mu^-) + p$ proceeds via $\gamma\gamma$ fusion. Again we avoid the odderon or $q\bar{q}$ exchange mechanisms. The QED $\gamma\gamma \to \ell^+\ell^-$ cross section can be calculated to good accuracy, and if we select events with very small p_{1t} of the leading proton, then the process may even be used to measure the incoming pp-luminosity [25, 26]. On the other hand, as p_{1t} increases the reaction becomes sensitive to the rapidity gaps survival factor $\hat{S}^2$. Hence, by varying the transverse momentum p_{1t} we may scan the proton-proton opacity $\Omega(b_t)$. The experimental problem is that to obtain a sufficient event rate we need to identify leptons (either muons or electrons) with transverse energy, E_T, as small as 1 or 2 GeV and large rapidity[8], $\eta \gtrsim 5$.

To illustrate the size of the effect we use a simplified form of the QED cross section, which corresponds to the limit $E_T \gg q_{1t}, q_{2t}$ and m, where q_i are the photon momenta and m is the lepton mass. After averaging over the azimuthal angle of the transverse momentum $\vec{E}_T$ of the lepton, the $\gamma\gamma \to \ell^+\ell^-$ subprocess amplitude squared is, see [26],

$$\frac{d\hat{\sigma}}{d\hat{t}} = \frac{\cosh(\Delta\eta)\pi\alpha^2}{4E_T^4 \cosh^4(\Delta\eta/2)} \times \Big(\Big\{ \Big((\vec{q}_{1t}\cdot\vec{q}'_{2t})(\vec{q}_{2t}\cdot\vec{q}'_{1t}) + (\vec{q}_{1t}\cdot\vec{q}'_{1t})(\vec{q}_{2t}\cdot\vec{q}'_{2t}) - (\vec{q}'_{1t}\cdot\vec{q}'_{2t})(\vec{q}_{1t}\cdot\vec{q}_{2t}) \Big) \Big/ \Big(q_{1t}q'_{1t}q_{2t}q'_{2t} \Big) \Big\} \Big) . \quad (33)$$

As before, we use q'_{it} to denote the photon transverse momenta in the complex conjugate amplitude. The relatively complicated form is associated with the polarisation vectors $\vec{\varepsilon}_i$ of the photons, which are parallel to the photon transverse momenta. Instead of a simple form like $\vec{\varepsilon}\cdot\vec{\varepsilon}'$, which occurred in J/ψ production, we now face correlations like $(\vec{\varepsilon}\cdot\vec{E}_T)(\vec{\varepsilon}'\cdot\vec{E}_T)$. After including all such terms, and averaging over the $\vec{E}_T$ direction we obtain (33). Recall that in the rescattering contribution the primed photon momenta $q'_{1t} = Q'_t - p'_{1t}$ of the complex conjugate amplitude, may differ from the momenta $q_{1t} = Q_t - p_{1t}$ occurring in the amplitude (and analogously for q'_{2t}), see Fig. 3a,b of [26]. In the absence of rescattering we put $Q = 0$ and/or $Q' = 0$. Finally, the cross section (33) has to be convoluted with the fluxes (4) for photons of momentum q_1 and q_2.

Sample results are presented in Fig. 10 for the LHC energy. The cross section has been integrated over the mass of the muon pair, with the cut $E_T > 4$ GeV on each muon. Again we see a clear diffractive dip at $-t = 0.2$ GeV^2 for the back-to-back proton configuration, $\phi = 180°$. Unfortunately the cross section is small and will make observation difficult.

In analogy to J/ψ production, it may be possible to measure only recoil proton and to observe the $\mu^+\mu^-$ pair, with $\vec{p}_{1t}$ reconstructed via $\vec{p}_{2t} + \vec{p}_{\mu^+\mu^- t}$. Here we can benefit from the high muon momentum resolution.

10 Conclusions

We have demonstrated that γ-exchange processes at hadron colliders (such as $pp \to p + M + p$) provide a good

[8] To measure small $p_{1t} \sim 100$ MeV we require $\xi_1 \gtrsim 0.03$. For the LHC it means that the longitudinal momentum of the lepton is $p_\parallel \sim \xi_1\sqrt{s}/4 \sim 100$ GeV. Thus the rapidity $\eta = -\ln\tan\theta/2 \simeq \ln(2p_\parallel/E_T) \sim 5$, and the polar angle of the lepton $\theta \simeq E_T/p_\parallel < 0.02$

testing ground for checking our ability to calculate the effects of rescattering, and in this way to scan the survival probability of rapidity gaps. We have taken the centrally produced system to be either the J/ψ vector meson or the W boson or a $\mu^+\mu^-$ pair. We have emphasized the important role played by photon polarisation; it may even reverse the sign of the absorptive corrections for small t and $\phi = 180°$ (where ϕ is the azimuthal angle between the transverse momenta of the two outgoing protons).

The interference between the pure γ exchange amplitude A^{γ} and the amplitude $A^{\gamma\mathbb{P}}$ with rescattering effects generates a rich diffractive structure of the differential cross section for processes of the type $pp \to p + M + p$. The tagging of both the leading protons, together with the centrally produced system, allows the rich t and ϕ dependence of the cross section to be measured. In this way the optical density of the proton-proton rescattering interaction can be probed as a function of the impact parameter.

For LHC energies, W boson production with a rapidity gap, looks the most promising probe of the gap survival probability. On the other hand, the J/ψ production process looks more realistic at RHIC energies (provided the background from $\chi \to J/\psi + \gamma$ can be supressed). Indeed a comparison of J/ψ and ϕ meson production also offers an attractive opportunity to search for odderon-exchange.

Acknowledgements. We thank Risto Orava and Krzysztof Piotrzkowski for interesting discussions. One of us (VAK) thanks the Leverhulme Trust for a Fellowship. This work was partially supported by the UK Particle Physics and Astronomy Research Council, by the Russian Fund for Fundamental Research (grants 01-02-17095 and 00-15-96610) and by the EU Framework TMR programme, contract FMRX-CT98-0194 (DG 12-MIHT).

References

1. V.A. Khoze, A.D. Martin, M.G. Ryskin, Eur. Phys. J. C **23**, 311 (2002)
2. Yu.L. Dokshitzer, V.A. Khoze, T. Sjöstrand, Phys. Lett. B **274**, 116 (1992)
3. J.D. Bjorken, Int. J. Mod. Phys. A **7**, 4189 (1992); Phys. Rev. D **47**, 101 (1993)
4. H. Chehime, D. Zeppenfeld, Phys. Rev. D **47**, 3898 (1993)
5. R.S. Fletcher, T. Stelzer, Phys. Rev. D **48**, 5162 (1993)
6. E.M. Levin, `hep-ph/9912402`; and references therein
7. V.A. Khoze, A.D. Martin, M.G. Ryskin, Eur. Phys. J. C **19**, 477 (2001); erratum, ibid C **20**, 599 (2001); and references therein
8. M.M. Block, F. Halzen, Phys. Rev. D **63**, 114004 (2001)
9. A.B. Kaidalov, V.A. Khoze, A.D. Martin, M.G. Ryskin, Eur. Phys. J. C **21**, 521 (2001)
10. V.A. Khoze, A.D. Martin, M.G. Ryskin, Eur. Phys. J. C **14**, 525 (2000)
11. V.A. Khoze, A.D. Martin, M.G. Ryskin, Eur. Phys. J. C **18**, 167 (2000)
12. E. Gotsman, E. Levin, V. Maor, Phys. Lett. B **353**, 526 (1995); Phys. Rev. D **60**, 094011 (1999); Phys. Lett. B **452**, 387 (1999);
13. V.A. Khoze, A.D. Martin, M.G. Ryskin, Phys. Rev. D **56**, 5867 (1997)
14. V.A. Khoze, A.D. Martin, M.G. Ryskin, hep-ph/0006005, in Proc. of 8th Int. Workshop on Deep Inelastic Scattering and QCD (DIS2000), Liverpool, eds. J. Gracey, T. Greenshaw (World Scientific, 2001) p.592
15. for reviews see, for example, V.M. Budnev, I.F. Ginzburg, G.V. Meledin, V.G. Serbo, Phys. Reports C **15**, 183 (1975); V.N. Baier, V.S. Fadin, V.A. Khoze, E.A. Kuraev, Phys. Reports, **78**, 293 (1981)
16. E710 Collaboration: N.A. Amos et al., Phys. Lett. B **247**, 127 (1990); CDF Collaboration: F. Abe et al., Phys. Rev. D **50**, 5518 (1994)
17. M.G. Ryskin, Z. Phys. C **57**, 89 (1993)
18. M.G. Ryskin, R.G. Roberts, A.D. Martin, E.M. Levin, Z. Phys. C **76**, 231 (1997)
19. L. Frankfurt, W. Koepf, M. Strikman, Phys. Rev. D **57**, 512 (1998)
20. H1 Collaboration: S. Aid et al., Nucl. Phys. B **472**, 3 (1996); H1 Collaboration: C. Adloff et al., Eur. Phys. J. C **10**, 373 (1999); Phys. Lett. B **483**, 23 (2000); ZEUS Collaboration: J. Breitweg et al., Z. Phys. C **75**, 215 (1997); Eur. Phys. J. C **6**, 603 (1999)
21. L. Lukaszuk, B. Nicolescu, Lett. Nuovo Cim. **8**, 405 (1973)
22. M.G. Ryskin, Yad. Fiz. **46**, 611 (1987); Sov. J. Nucl. Phys. **46**, 337 (1987); J. Czyzewski, J. Kwiecinski, L. Motyka, M. Sadzikowski, Phys. Lett. B **398**, 400 (1997)
23. R.A. Janik, J. Wosiek, Phys. Rev. Lett. **82**, 709 (1999); M.A. Braun, P. Gauron, B. Nicolescu, Nucl. Phys. B **542**, 329 (1999); J. Bartels, L.N. Lipatov, G.P. Vacca, Phys. Lett. B **477**, 178 (2000)
24. S.J. Brodsky et al., Phys. Rev. Lett. **93**, 451 (1980); S.J. Brodsky, C. Peterson, N. Sakai, Phys. Rev. D **23**, 274 (1981)
25. A.G. Shamov, V.I. Telnov, in Forward Physics and Luminosity Determination at LHC, eds. K. Huitu et al., (World Scientific, Singapore), p.136 (2001)
26. V.A. Khoze, A.D. Martin, R. Orava, M.G. Ryskin, Eur. Phys. J. C **19**, 313 (2001)